Physics-Informed Neural Networks with New Activation Function and Multi-Objective Optimization for Improving Estimation of Soil Hydraulic Properties

Jize Fan[1], Xiaofei Yan[2], Qiang Cheng[1,3*]

[1]College of Information and Electrical Engineering, China Agricultural University, 100083 Beijing, China

[2]School of Technology, Beijing Forestry University, Beijing 100083, China

[3]State Key Laboratory of Efficient Utilization of Agricultural Water Resources，Beijing, China

Key Points:

Soil matric potential was more precisely estimated from added sparse calibration points

Incorporating a new strategy into optimizing the multi-objective loss function

Saturated hydraulic conductivity was introduced into the activation function as an optimizable prior knowledge

Abstract

While physics-informed neural networks (PINNs) can solve the problem pertaining to the absence of boundary conditions in soil water systems, their results exhibit low accuracy primarily due to insufficient utilization of the available prior knowledge regarding soil hydraulic parameters. In this research, an improved PINNs framework is proposed, which introduces an optimizable saturated hydraulic conductivity into the activation function, and an advanced optimization strategy is developed to identify the optimal superparameters for the multi-objective loss function. The PINNs was trained using synthetic volumetric soil water content (VSWC) and soil matric potential (SMP) data generated by a numerical solution of the Richardson-Richards equation (RRE) for three soil types (silt loam, loam and sandy loam). The results show that the proposed framework increases the accuracy of SMP estimations in the unsaturated soil system. The results reveal that the relative error achieved by the proposed framework in loam or silt loam has been reduced by two orders of magnitude in comparison with that achieved by the framework introduced by Bandai and Ghezzehei (2020), indicating a significant improvement. While there is a slight reduction in the accuracy of volumetric soil water content estimation, this minor reduction has minimal practical significance. Both the soil water retention curve and the soil hydraulic conductivity exhibit superior performance at the near-saturation scale. For unsaturated flow in homogeneous soil, the proposed PINNs framework provides accurate estimations of soil hydraulic parameters and holds significant potential for the practical application and widespread adoption of PINNs in the realm of soil hydrodynamics.

1. Introduction

Numerical simulation modelling of water flow in saturated-unsaturated soil systems is an important method to promote a quantitative understanding of hydrological processes, which is crucial for remote sensing, weather forecasting, irrigation management, natural disaster prediction, etc. (Babaeian et al., 2019; Robinson et al., 2008). The study of soil hydrodynamics frequently relies on the numerical solution of differential equations, employing both the finite difference method and the finite element method. (Chávez-Negrete et al., 2018; Yazdchi, Khalili, & Valliappan, 1999).

Despite significant progress, traditional analytical and computational tools still face enormous challenges due to high computational costs and uncertainties (Assouline, 2006; Durner et al., 2008; Saito et al., 2006). These uncertainties include complex formulas, new algorithms, and sophisticated computer codes, as well as missing boundary conditions and significant errors in observations (Bitterlich et al., 2004; Carrera et al., 2005; Scanlon, et al., 2003, Raissi et al., 2019; Raissi et al., 2020).

PINNs are a numerical simulation algorithm that has rapidly developed in recent years (Cai et al., 2021). They fit specific solutions to partial differential equations (PDEs) using neural networks. The loss function of the neural network consists of two parts, the observation error and the PDEs error, which allows PINN to fit a special solution of known physical knowledge from the measurement data. This new approach works well in computational physics.

It is worth noting that Tartakovsky et al. (2020) only used soil matric potential data at observation sites and PINNs to estimate soil hydraulic properties (hydraulic conductivity functions (HCF) and water retention curves (WRC)) for unsaturated homogeneous soils. Bandai & Ghezzehei (2021) introduced a priori knowledge into the model structure and used two monotonic neural networks to estimate the WRC and HCF of the system, only using soil moisture content data to simulate soil moisture dynamics. Shi et al. (2022) replaced the known priori physical information with sparse regression and simulated the homogeneous soil moisture transport process under the boundary of evaporation and precipitation only using soil moisture content data. Shi et al. (2023) also found that hydrothermal coupling physical constraints improved the accuracy of soil hydraulic parameter estimation. PINNs were validated in complex 2D groundwater flow scenario (Wang et al., 2020). PINNs were used to perform a joint inversion in a steady-state advection-dispersion problem to simulate the conductivity, soil matric potential and concentration of the system and to estimate the parameters in the system. (He et al., 2020). The methods described above all use datasets generated from the results of hydrological model simulations. The estimation accuracy of PINNs was also validated by using measured volumetric water content (VSWC) from soil column infiltration experiments. (Depina et al., 2022)

The focus of the above algorithm is to estimate soil hydraulic parameters using water potential or volumetric water content, combined with a priori knowledge. As sensor network measurements as infrastructure are more convenient and accurate, Yu et al. (2021) developed automated sampling devices that can simultaneously measure soil profile moisture and soil matric potential. PINNs need to adapt to the development of automated collection devices to utilize diverse measurement data. The diversity of measurement data advances optimization methods. Multi-task learning is representative, and its innovation is to automatically assign the weights of multiple objective functions to improve the generalization of the model (Zhang & Yang, 2018). The automatic assignment of weights for physical information loss and calibration point loss can improve the robustness and convenience of PINNs.

Interfaces are needed in the algorithm to encode a priori knowledge based on historical observations and measurements into the optimizing algorithm. For example, adding physical information loss to the objective function is the underlying principle of PINNs (Raissi et al., 2019; Yang et al., 2019; Yang & Perdikaris, 2019; Zhao et al., 2019; Zhu et al., 2019). Parameters are initialized with positive constraints to restrain the WCF and the WRC monotonically. Activation functions are important elements of neural networks, and they mainly play a role in introducing nonlinear transformations for each neuron in the network, thus enabling the neural network to learn and express more complex functional relationships (Apicella et al., 2021). Research on activation functions has focused on improving the robustness of optimization algorithms. The introduction of optimizable parameters in the activation function allows PINNs to incorporate more physical information and improve the estimation accuracy of models.

In this paper, we will make enhancement based on the study of Bandai et al (Bandai & Ghezzehei, 2021). Firstly, we add the soil matric potential calibration points to reduce the error of the soil matric potential estimation. We also propose a new s-type activation function that incorporates the shape prior knowledge of the Van Genuchten (VG) model into the model architecture, and demonstrate the effectiveness of the model by comparing it with the original version. The framework's performance was investigated by randomly initializing the neural network parameters on the generated training set data, repeating the experiment 30 times, and calculating the confidence interval of the results. To investigate the generalizability of the framework, PINN was trained on data from three different soil types (loam, sandy loam, and silt loam).

2. Background

2.1. Soil Moisture Transport Equation

The Richardson-Richards Equation describes the movement of soil water in unsaturated soils. This quasilinear partial differential equation is fundamental for understanding water flow in porous media under variably saturated conditions.

$$\frac{\partial\theta(\psi(t,z))}{\partial t} = \frac{\partial}{\partial z}\left[K\big(\psi(t,z)\big)\left(\frac{\partial\psi(t,z)}{\partial z}+1\right)\right] \tag{1}$$

where t is time [T]; z is the vertical coordinate (positive upward) [L]; θ is the volumetric water content [L^3 L^{-3}]; ψ is the soil matric potential [L]; The functions K(ψ) and θ(ψ) are called hydraulic conductivity functions (HCF) and water retention curves (WRC) respectively.

2.2 Neural networks and the Error Backpropagation Algorithm

Neural networks, inspired by the human brain, are powerful models used in machine learning (Goodfellow et al., 2016). Artificial neural networks are composed of interconnected nodes, which are organized into layers. These layers include an input layer, one or more hidden layers, and an output layer. These networks learn from data by adjusting their internal parameters, namely weights and biases, to make accurate predictions or classifications. Backpropagation is a crucial process in neural network training (Wythoff, 1993). It fine-tunes the weights based on the error (loss) obtained during forward propagation. During forward propagation, input data is passed through the network. The error representing the difference between the predicted and actual results will be calculated. In back-propagation, this error is propagated backwards through the layers and the weights are adjusted to minimize the error. The goal is to find optimal weights that lead to lower error rates, thereby improving the generalization of the model. The input to the PINNS is not the features of the output, but the coordinate system of the partial differential equations. During error back propagation, the differential numerical solution for the corresponding grid of the output is computed while propagating one step forward.

"Physics Information Neural Networks" (PINNs) are machine learning algorithms that combine data and prior knowledge, such as differential equations and parameters, to improve interpretability and convergence even with imperfect data (Raissi & Karniadakis, 2018; Raissi et al., 2019). This results in physically consistent and accurate predictions. PINNs encode prior knowledge into components like the loss function of machine learning.

3. Methods

This paper uses physics-informed neural networks (PINNs) to obtain the solution of the Richards' equation (RRE) and soil hydraulic parameters from time series data of VSWC and SMP at various depths. Figure 1 illustrates the network structure, which comprises three fully connected neural networks. The neural network (fig. 1a) maps the system's coordinates t and z to the SMP. The hidden layer uses the hyperbolic tangent function as its activation function, while the output layer uses a negative exponential function to ensure a negative output SMP. In practice, neural network (fig. 1b) is used to estimate hydraulic conductivity K and its output layer activation function is shown in Figure 2. Various soil hydraulic parameters correspond to different parameters c. A neural network (fig. 1c) is employed to estimate VSWC. The output layer also utilizes a new activation function. The value of parameter γ is 1. The SMP output by the neural network (fig. 1a) is converted to a logarithmic scale, which makes it easier to draw WRC and HCF diagrams, and can also reduce the SMP fitting error in the loss function. The logarithmic scale estimate of soil matrix potential was used as input to two neural networks to map hydraulic conductivity K and VSWC. The new activation function makes changes based on the sigmoid function, which contains some of the properties of the sigmoid function, such as the output value is positive and ranges from 0-1, and his parameter γ improves the fitting performance of the neural network in the arid region.

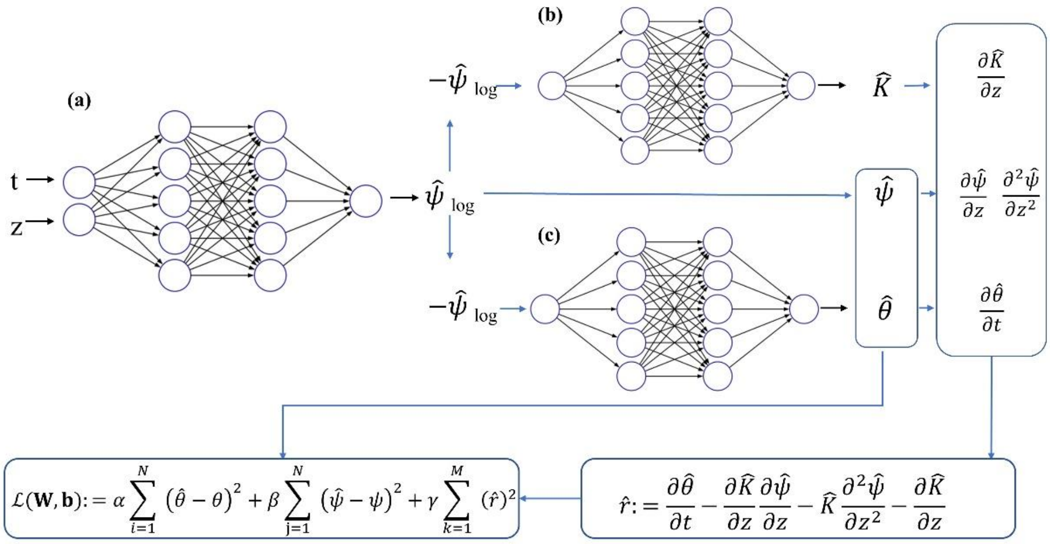

Figure 1. A physical information neural network (PINNs) is employed to estimate the specific solution of the Richardson-Richards equation (RRE), using a new activation function. The network comprises three parts, which are used to fit the hydraulic conductivity, soil matric potential (SMP), and volumetric soil water content (VSWC). The loss function has a hyperparameter in front of each item to adjust the focus of the fitting.

To incorporate a priori knowledge of the VG model, an activation function is introduced to improve the estimation accuracy of hydraulic parameters in the saturated and arid zones. The activation function is as follows:

$$\sigma(z) = a\left(\frac{1}{1+e^{-(z-b)}}\right)^{c} \tag{2}$$

The parameter a may refer to either the saturated hydraulic conductivity or the saturated water content. The position of the center of symmetry of the S-curve is controlled by parameter b. The steepness of the low value region is controlled by parameter c. The image of the activation function is shown in Figure 2.

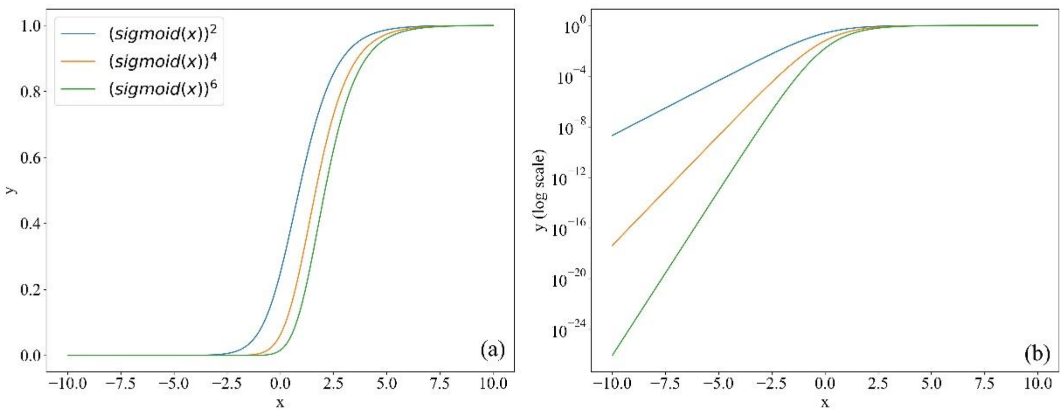

Figure 2. (a) Illustration of the activation function, (b) Illustration of the activation function in logarithmic scale.

Integrating multi-source data into existing models remains a challenge in practice, as it requires complete and accurate data. It is essential to develop a new approach that can identify multi-dimensional correlations, unify the multi-scale modelling process and reduce the difficulty of parameter estimation (Karniadakis et al., 2021). The parameter set of the neural network is solved by minimizing the objective function, and the loss function is:

$$\mathcal{L}(\boldsymbol{W}, \boldsymbol{b}) := \alpha \sum_{i=1}^{N} (\hat{\theta} - \theta)^2 + \beta \sum_{j=1}^{N} (\hat{\psi} - \psi)^2 + \gamma \sum_{k=1}^{M} (\hat{r})^2 \tag{3}$$

The loss function comprises of three terms. The first two terms represent the fitting error of the VSWC and soil SMP, while the third term represents the constraint imposed by the partial differential equation. The coefficients of the activation function are represented by α, β, and γ.

Other studies on PINNs have also introduced boundary and initial conditions for PDEs in the objective function. Bandai's experiments have shown that PINNs can fit the specific solution of RRE and soil hydraulic parameters if a large enough data set of VSWC time series is provided without introducing boundary conditions and initial conditions. PINNs use automatic differentiation to calculate the derivatives of partial differential equations. The residuals of a partial differential equation can be computed in an arbitrary domain, which means that we can reduce the complexity of the loss function by controlling the size of the residuals of the partial differential equation. A grid that is denser than the sampling points is used, with spatial spacing of 5 cm and temporal spacing of 0.1 days. Prior to training the PINNs in this study, weight parameters W were initialized through a uniform distribution, and bias of nodes were set to zero. Next, these parameters were trained by optimizing the loss function. The hyperparameters in the loss function are critical to the PINNs because an accurate fit of the VSWC and SMP is the basis for estimating soil hydraulic parameters. However, the weights of the physical PDEs constraints are not easy to determine. Since the physical constraints and fitting errors are of different orders of magnitude, their impact on the neural network varies greatly. When there are multiple constraints, it is a challenge to adjust the weight coefficients. The annealing training method based on gradient learning rate proposed by Wang et al. balances multiple constraints by controlling the coefficients of the physical PDEs constraints (Wang et al., 2023). In our work, we draw on this idea to balance two physical constraints. We take the physical constraint with the smallest order of magnitude as the baseline and adjust the coefficients so that the orders of magnitude of the VSWC and SMP fitting errors are the same as the orders of magnitude of the physical constraints. The determination of the coefficients generally requires multiple rounds of iterations, with the coefficients of the soil matric potential fitting error doubling at the end of each round of training until the HCF and the WRC are not smooth. Our first step is running the Adam optimizer in Pytorch for 120,000 iterations using its default settings and setting the decay rate to 0.99. We then fine-tune the parameters using the L-BFGS-B algorithm to minimize the objective function.

To ensure monotonicity of the WRC and HCF, the parameters of the fully connected layers of the neural networks (b and c) are initialized to small positive numbers, e.g. 0.05. This ensures that the neural networks b and c fit into monotonically increasing functions and correspond to the physical properties of the soil water movement.

HYDRUS-1D was used to generate the VSWC and SMP. The artificial data were used to (1) study the adaptive weight loss function algorithms and (2) investigate the generalizability of the PINNs. The HYDRUS-1D simulated system dynamics for 25 days covering 100 cm of three different homogeneous soils (loam, sandy loam and silty loam). The soil column was uniformly discretized at 0.1 cm grid spacing. The initial VSWC was chosen to vary linearly from 15% to 25% from the top to the bottom for each depth. The Neumann boundary condition is used as the lower boundary condition, while the upper boundary condition is the time-varying atmospheric upper boundary condition. Table 1 displays the VG model parameters for the three soils used in the numerical simulation.

Table 1. Van Genuchten(VG) model parameters for three soil types.

VG model parameters	Silt Loam	loam	Sandy loam
θ_r [cm^3 cm^{-3}]	0.067	0.078	0.065
n [-]	1.41	1.56	1.89
K_s [cm day^{-1}]	10.8	24.96	106.1
α [cm^{-1}]	0.02	0.036	0.075
θ_s [cm^3 cm^{-3}]	0.45	0.43	0.41

To assess the PINNs performance, we calculated the relative errors of the true and predicted SMP, VSWC, soil water flux density (SWFD) and hydraulic conductivity. We quantized the prediction error over time t $\in$ [0, 25] days and spatial domain z $\in$ (-100, 0] cm for all four of them as relative L_2 errors defined as:

$$\epsilon^{\gamma} := \frac{\sum_{t\in[0,25]} \sum_{z\in(-100,0]} (\hat{\gamma}(t,z) - \gamma(t,z))^2}{\sum_{t\in[0,25]} \sum_{z\in(-100,0]} \gamma(t,z)^2} \qquad (4)$$

To demonstrate the effectiveness of the improved PINNs, we also trained the original PINNs (i.e. without the new activation function and error adaptation) with the same training data for comparison.

4 Results and Discussions

4.1 Neural Network Architecture in Physics-Informed Neural Networks

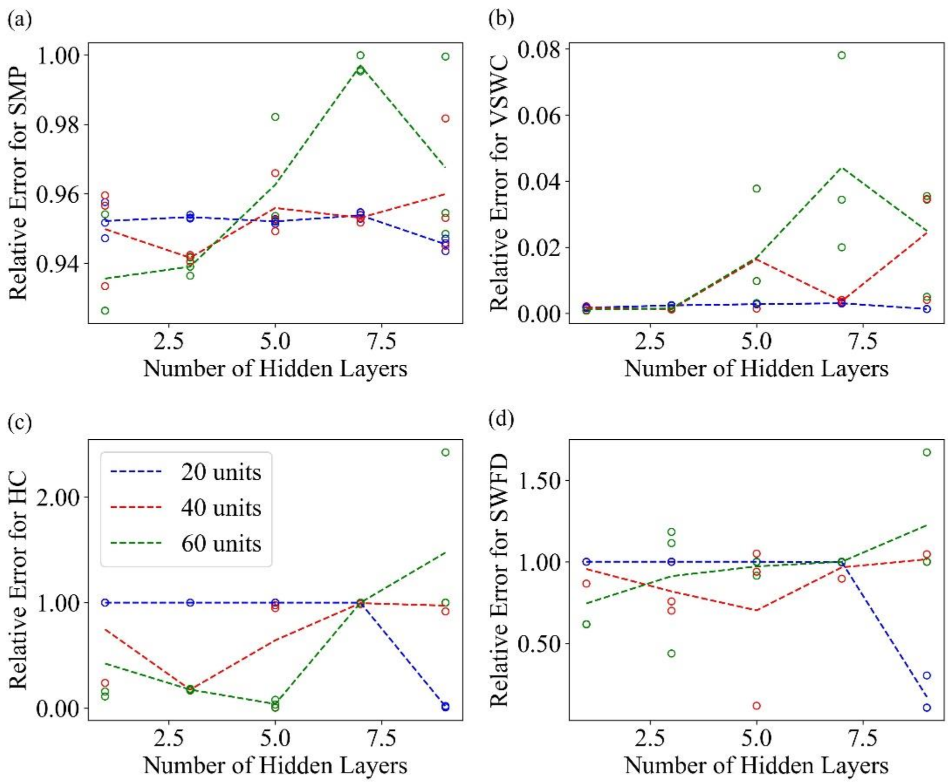

Figure 3. The relative errors ϵ of the (SMP), VSWC, soil water flux density (SWFD) and hydraulic conductivity (HC) change with different hidden layers and unit numbers of the neural network. The three neural networks are designed to change simultaneously. The lines represent the average of three repeats of each net structure.

The number of neural network hidden layers and units in the PINNs with the new activation function was tested by exploring different combinations of layers and units. The trend of the relative error ϵ for SMP, hydraulic conductivity, VSWC, and SWFD for varying numbers of hidden layers and units of the neural networks is shown in Fig. 3. The structure of the three neural networks was changed synchronously.

The relative errors of soil matric potential, volumetric water content, soil water flux density, hydraulic conductivity, and for the PINNs using the new activation function do not follow the same trend as the number of cells increases. As the number of hidden layers increases, the relative errors of SMP and VSWC increase and then decrease. The relative error of hydraulic conductivity, on the reverse, decreases and then increases, while the relative error of soil water flux always increases at a hidden layer number of 60. When the number of hidden layer units is 10, the relative errors of SMP and VSWC remain almost unchanged, and the relative errors of hydraulic conductivity and soil water flux change very little at the beginning and decrease at the end. When there are 40 hidden layer cells, the relative errors of SMP and VSWC fluctuate, and the relative errors of hydraulic conductivity and soil water flux decrease initially and increase at the end, but the minimum mean is not the same as in the hidden layer. A nonlinear correlation was found between the relative errors of hydraulic conductivity, SWFD and VSWC and the number of hidden layers. When the number of hidden layers of soil matric potential is 3, the number of hidden layers of VSWC is 1, the number of hidden layers of hydraulic conductivity K is 5 and the number of hidden layers of SWFD is 9, the mean relative error is the lowest.

To enhance the algorithm's robustness, we utilize various random number seeds to initialize the network and compute the range of relative error variation. We excluded all network structures when the hidden layer unit was 60, the relative errors of SMP and VSWC were very unstable when the hidden layer was more than 5. There was no noticeable improvement in the relative errors when the hidden layer was less than 5, compared to a hidden layer unit of 40. Reducing the hidden layer number further demonstrates the benefits of improving the stability of the optimizing. It was observed that when the hidden layer units are very small, the relative errors in hydraulic conductivity and SWFD remain large until the number of hidden layers reaches 9. This is attributed to the fact that the hidden layer units are too small to represent the non-linear relationships in the dataset. When the hidden layer units of the neural network were fixed, the relative errors in hydraulic conductivity, VSWC and SMP were minimal at 3 hidden layers. In summary, the structures of the PINNs are defined as shown below: neural networks consist of 3 hidden layers and 40 units.

However, the performance of PINNs using the new activation function is sensitive to the neural network structure. Therefore, we recommend optimizing the network structure again after changing the data set or loss function to improve the model's accuracy.

4.2 Generalization Ability of PINNs

Data-driven algorithms can accurately fit data, but their poor generalization often leads to inaccurate predictions or a failure to learn the intrinsic relationships within the data (Shen et al., 2023). The PINNs' generalization capability was evaluated using synthetic data derived from HYDRUS-1D with the new activation function and monotonicity constraints. Table 2 displays the relative error for SMP ($\epsilon\psi$), hydraulic conductivity (ϵK), VSWC ($\epsilon\theta$), and SWFD (ϵq). The newly proposed PINNs can be identified by the small values of the relative error for the soil matric potential $\epsilon\psi$ and the large values for the VSWC $\epsilon\theta$. Both models performed well in terms of relative error for hydraulic conductivity and SWFD. This is mainly due to the soil matric potential data in the training dataset, which can be well handled by the newly proposed PINNs, as shown in Figure 1. Thus, the subsequent sections will concentrate on the outcomes for PINNs using the new activation function.

Table 2. Relative error (mean (± standard deviation)) of PINNs trained from VSWC and SMP for soil matric potential $\epsilon\psi$, volumetric water content $\epsilon\theta$, soil water flux density ϵq and hydraulic conductivity ϵK.

Relative error	Silt loam	Loam	Sandy loam
PINNs with new activation function using VWC and SMP			
ϵ^{θ}	1.56(±0.92)×10^{-3}	1.25(±0.52)×10^{-3}	7.56(±1.26)×10^{-4}
ϵ^{ψ}	9.43(±0.03)×10^{-1}	9.82(±0.01)×10^{-1}	9.95(±0.03)×10^{-1}
ϵ^{K}	2.07±1.84)×10^{-1}	5.42(±1.08)×10^{-1}	2.90(±1.88)×10^{-2}
ϵ^{q}	8.01(±2.98)×10^{-1}	3.24(±0.34)×10^{-2}	1.35(±1.02)×10^{-2}

PINNs with monotonicity constraints using VWC			
ϵ^{θ}	5.86(±0.67)×10^{-5}	3.36(±0.49)×10^{-5}	4.27(±0.45)×10^{-5}
ϵ^{ψ}	3.37(±0.91)×10^{1}	7.65(±2.54)×10^{2}	9.71(±0.25)×10^{-1}
ϵ^{K}	6.32±5.64)×10^{-1}	2.38(±0.62)×10^{-2}	1.52(±9.86)×10^{-2}
ϵ^{q}	1.03(±3.50)×10^{-1}	2.16(±4.01)×10^{-2}	2.69(±7.65)×10^{-2}

4.2.1 Soil Matric Potential and Volumetric Soil Water Content

Figure 4 illustrates the VSWC predicted by the PINNs for the sandy loam soil using the new activation function. The training data allowed the PINNs to accurately capture the actual pattern of soil moisture motivation. However, larger errors were observed when the initial conditions changed suddenly. This suggests that the neural networks were unable to capture such drastic changes in soil moisture dynamics. Following rainfall, the upper boundary conditions change, resulting in predicted values that are smaller than the true values. This could be due to insufficient data or the fact that surface soil moisture dynamics are not solely driven by RRE. The soil matric potential also shows a similar trend, as shown in Figure 5.

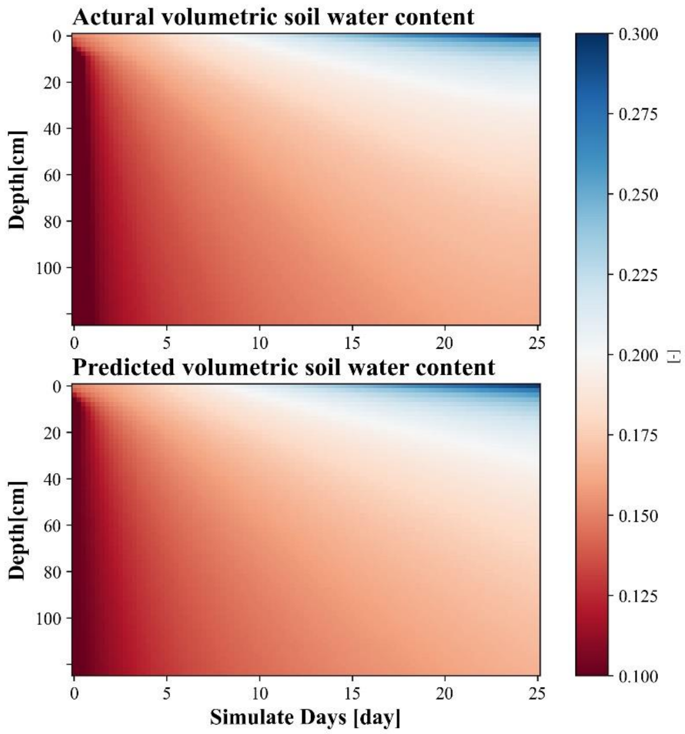

Figure 4. Simulated and real spatiotemporal volumetric soil water content distributions in sandy loam.

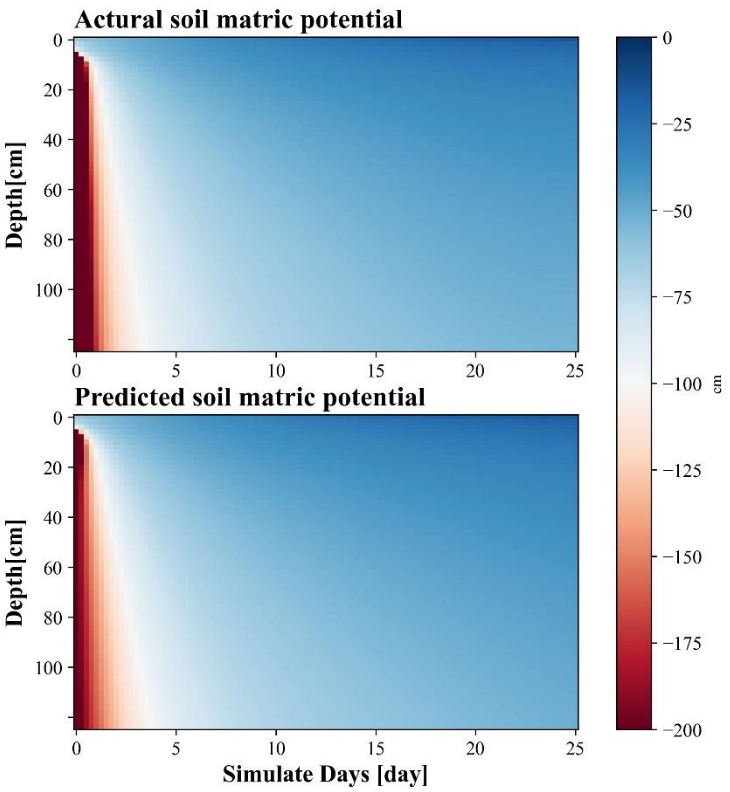

Figure 5. Simulated and real spatiotemporal soil matric potential distributions in sandy loam.

4.2.2 Soil Water Retention Curves

The study evaluates the ability of PINNs, with a new activation function, to estimate soil hydraulic properties. The use of moisture and substrate potential data from different sites to estimate soil water retention curves was one of the original aims of the paper. As previously stated, the PINNs model with monotonicity constraints provides inadequate predictions for the WRC at both the near-saturated and drought scale due to the limited estimation of parent potential. In particular, the outcomes for low and high VSWC were not good. As Figure 6 shows, the predicted water retention curves of sandy loam and loam are similar to the actual water retention curves, whether in arid or saturated areas. The water retention curve prediction for silty loam soil has the largest error in the near-saturated zone. This may be due to insufficient data in these ranges or because the special solution of RRE at the near-saturated is not smooth. Wang et al. (2023) reported similar observations where the soil matric potential was accurately estimated using VSWC and soil temperature data through the use of PINNs derived from the coupled soil-hydrothermal model.

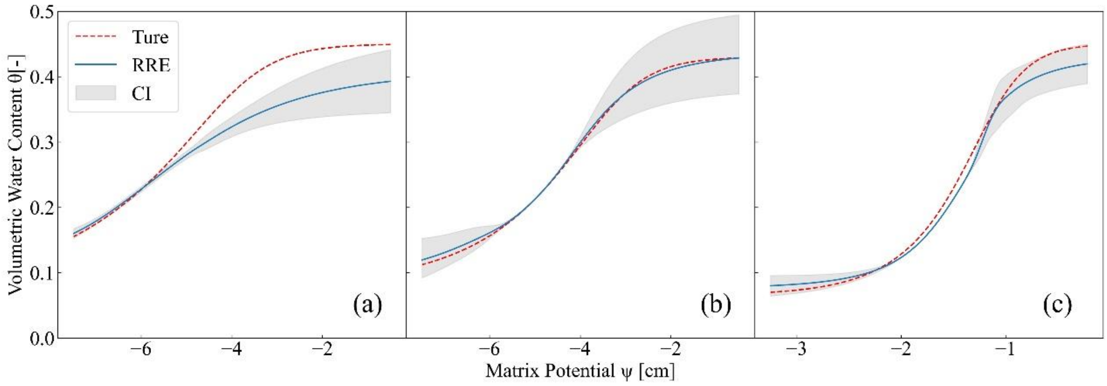

Fig. 6. Water retention curves (true) for three soils compared to those predicted by PINNs using the new activation function. WRCs for (a) silt loam, (b) loam, and (c) sandy loam. Grey shaded areas are confidence intervals taken as the mean plus or minus three times the standard deviation after 30 replications.

4.2.3 Hydraulic Conductivity Functions

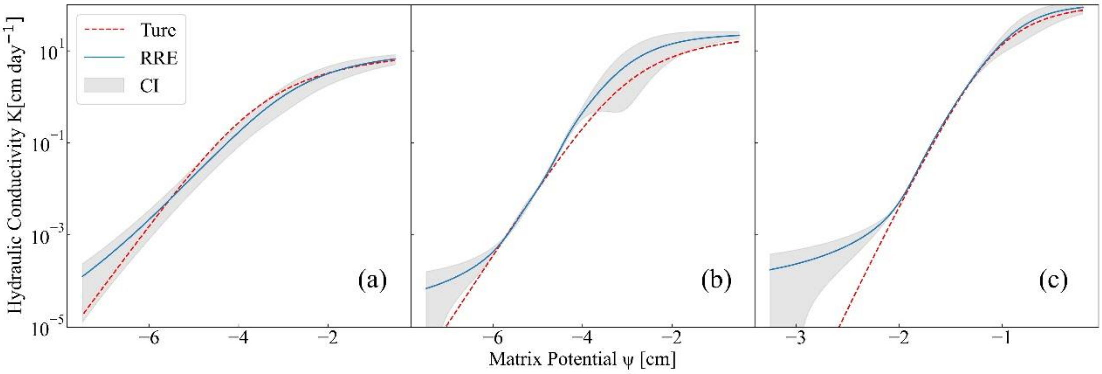

Fig. 7. Hydraulic conductivity functions of three soils compared with those predicted by the new activation function of PINNs. HCFs for (a) silt loam, (b) loam, and (c) sandy loam. Grey shaded areas are confidence intervals taken as the mean plus or minus three times the standard deviation after 30 replicates. The lower confidence interval for loam is 2.5 times the standard deviation, rather than three times, to avoid negative values that would distort the image on the log scale.

The predicted HCFs for the three soils are shown in Figure 7. The estimated hydraulic conductivity function of the silt loam is similar to the actual hydraulic conductivity function, whether in dry or saturated areas. The monotonic constraint is insufficient to represent the strong nonlinearity of HCF and does not provide enough data on the humidity scale. To address this issue, we introduce a priori saturated hydraulic conductivity and saturated water content. It is important to note that the prior knowledge must be within a suitable range, otherwise PINNs convergence will not be achieved. Sandy loam and loam soils exhibit the greatest error in HCF under dry conditions. The PINNs using the new activation function can estimate the HCF, especially in the middle range. However, it is not possible for PINNs to accurately estimate the HCF at the dry scale. The dry data are concentrated in the surface 5 cm range, and since the data are sparse, the training data are poorly distributed in this range and do not help to learn the HCF in the dry range. Depina et al. (2022) found that hydraulic conductivity in the intermediate range can be estimated from soil matric potential or VSWC. The method proposed in this paper does not reduce the residuals of the RRE, but only distributes the residuals uniformly over all the estimated features, which is shown by the increase in the relative error of the VSWC and the decrease in the relative error of the SMP. In order to promote the application of PINNs in the field of soil moisture dynamics simulation and to adapt the sampling method to the existing sensor networks, the algorithm provides more optimizable parameters such as saturated hydraulic conductivity, saturated water content. Compared to other methods of estimating hydraulic conductivity, the PINNs method has the advantages of being able to use a priori information about the HCF, such as saturated hydraulic conductivity.

4.2.4 Soil Water Flux Density

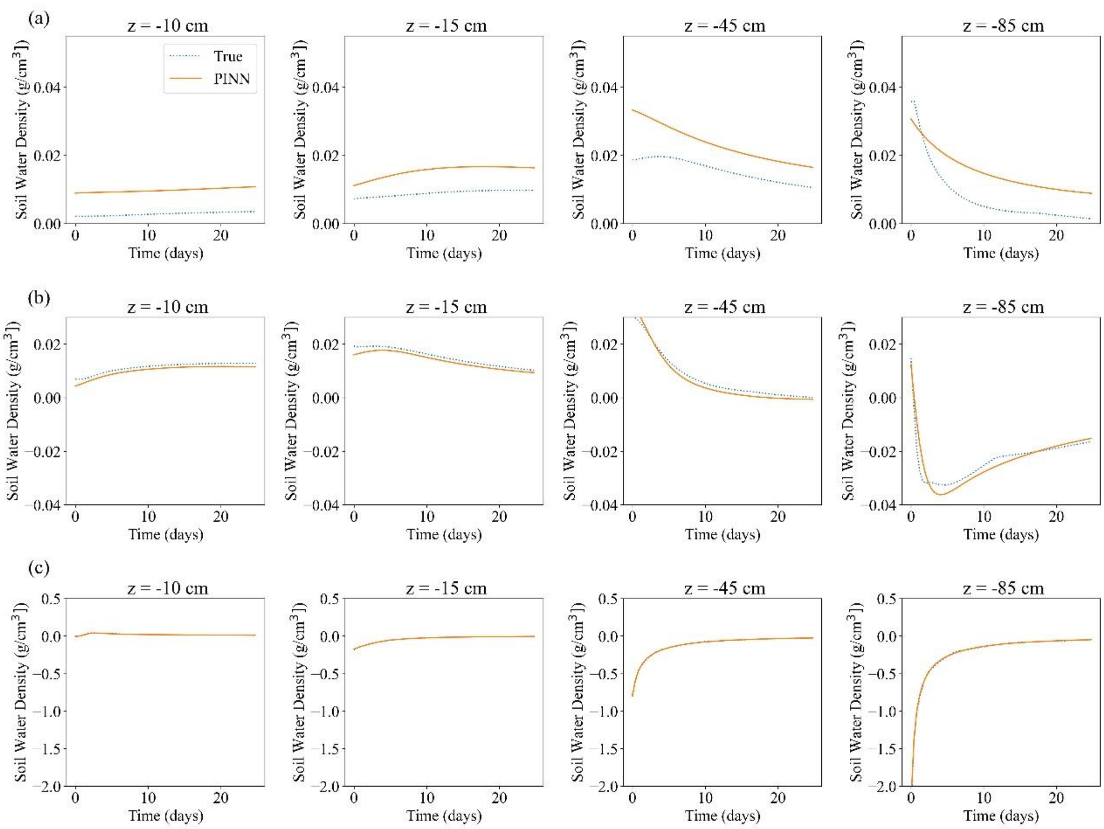

Figure 8. Estimated versus true soil water flux density values for (a) silt loam, (b) loam, (c) sandy loam at four different depths. z = -10 cm, z = -15 cm, z = -45 cm, and z = -85 cm.

The performance of the PINNs framework in estimating SWFD will be tested. Figure 8 presents a comparison between the estimated and true soil water flux density at four depths (z = -1, -15, -45, -85 cm) in sandy loam. Rapid changes in soil water flux density and large errors were found near the wetting front and at the surface. Despite the relatively high errors for loam and silt loam, the PINNs with the new activation function adequately represents the pattern of SWFD, as illustrated in Figure 8.

The potential of the PINNs approach to estimate soil evaporation from subsurface soil measurements in the field is significant. The widespread availability of sensors and the decreasing manufacturing costs have resulted in the accumulation of a large amount of usable observational data (collected or generated), which are crucial for mathematical modelling (Jackson et al., 2008; Kamai et al., 2008). This can be achieved through continuous measurements of SMP and VSWC using mobile FDR sensors (Yu et al., 2021) and pipeline robots (Yan et al., 2023), which are becoming increasingly popular. Therefore, this approach is important for applications in surface modelling (e.g. Sadeghi et al., 2020) and agricultural engineering (Umutoni & Samadi, 2024).

5 Summary and Conclusions

This paper proposes a new framework that uses Physics-Informed Neural Networks (PINNs) to estimate soil hydraulic parameters, specifically the WRCs and HCFs, from limited VSWC and SMP measurements. The saturated hydraulic conductivity was introduced into the neural network through a parameterized S-type activation function. Therefore, our framework is more practical for modelling soil moisture dynamics. To assess the capabilities of the new framework, its comparison with the original PINNs was carried out. The PINNs were trained using datasets from three different soil characteristics (loam, sandy loam and silty loam). The generalizability of the framework, i.e. the ability to estimate WRC, HCF and SWFD, was tested. PINNs with a new activation function can estimate the true soil water dynamics from various types of synthetic soil data. In regards to soil water holding curves, PINNs with a new activation function performs worse in estimating the near-saturated scale of silt loam and better in estimating the sandy loam and loam. In contrast to WRC, PINNs with the new activation function can predict the HCF of silt loam well, but performs worse on the dry scale. The results suggest that the model estimation accuracy can be improved by using the new activation function and adding soil matric potential calibration points in PINNs. This approach has the advantage of not requiring initial and boundary conditions, and can leverage more prior knowledge.

Acknowledgments

This study is supported by the National Natural Science Foundation of China (32271990) and National Key Research and Development Program (2023YFD2301101-01). We are indebted to anonymous reviewers for improving this manuscript.

Open Research

Data Availability Statement

The dataset (Fan, 2024a) and code (Fan, 2024b) used in this study are available. The dataset is from numerical simulations and the original files are published on github https://github.com/fgzml/Physics-Informed-Neural-Networks-with-New-Activation-Function.git (Fan, 2024a) The software associated with this manuscript is licensed under MIT. Figures were made with Matplotlib version 3.2.1 (Caswell et al., 2020; Hunter, 2007), available under the Matplotlib license at https://matplotlib.org/.

References

Apicella, A., Donnarumma, F., Isgrò, F., & Prevete, R. (2021). A survey on modern trainable activation functions. Neural Networks, 138, 14-32. https://doi.org/https://doi.org/10.1016/j.neunet.2021.01.026

Assouline, S. (2006). Modeling the relationship between soil bulk density and the hydraulic conductivity function. Vadose Zone Journal, 5(2), 697-705. https://doi.org/10.2136/vzj2005.0084

Babaeian, E., Sadeghi, M., Jones, S. B., Montzka, C., Vereecken, H., & Tuller, M. (2019). Ground, Proximal, and Satellite Remote Sensing of Soil Moisture. Reviews of Geophysics, 57(2), 530-616. https://doi.org/10.1029/2018rg000618

Bandai, T., & Ghezzehei, T. A. (2021). Physics-Informed Neural Networks With Monotonicity Constraints for Richardson-Richards Equation: Estimation of Constitutive Relationships and Soil Water Flux Density From Volumetric Water Content Measurements. Water Resources Research, 57(2), 20. https://doi.org/10.1029/2020wr027642

Bitterlich, S., Durner, W., Iden, S. C., & Knabner, P. (2004). Inverse estimation of the unsaturated soil hydraulic properties from column outflow experiments using free-form parameterizations. Vadose Zone Journal, 3(3), 971-981. https://doi.org/10.2113/3.3.971

Cai, S., Mao, Z., Wang, Z., Yin, M., & Karniadakis, G. E. (2021). Physics-informed neural networks (PINNs) for fluid mechanics: A review. Acta Mechanica Sinica, 37(12), 1727-1738. https://doi.org/10.1007/s10409-021-01148-1

Carrera, J., Alcolea, A., Medina, A., Hidalgo, J., & Slooten, L. J. (2005). Inverse problem in hydrogeology. Hydrogeology Journal, 13(1), 206-222. https://doi.org/10.1007/s10040-004-0404-7

Caswell, T., Droettboom, M., Lee, A., Hunter, J., Firing, E., Stansby, D., et al. (2020). Matplotlib v3.2.1 [Software]. Zenodo. https://doi.org/10.5281/zenodo.3714460

Chávez-Negrete, C., Domínguez-Mota, F. J., & Santana-Quinteros, D. (2018). Numerical solution of Richards' equation of water flow by generalized finite differences. Computers and Geotechnics, 101, 168-175. https://doi.org/10.1016/j.compgeo.2018.05.003

Depina, I., Jain, S., Valsson, S. M., & Gotovac, H. (2022). Application of physics-informed neural networks to inverse problems in unsaturated groundwater flow. Georisk-Assessment and Management of Risk for Engineered Systems and Geohazards, 16(1), 21-36. https://doi.org/10.1080/17499518.2021.1971251

Durner, W., Jansen, U., & Iden, S. C. (2008). Effective hydraulic properties of layered soils at the lysimeter scale determined by inverse modelling. European Journal of Soil Science, 59(1), 114-124. https://doi.org/10.1111/j.1365-2389.2007.00972.x

Fan, J. (2024a). Datasets from hydrus simulations for three soils [Dataset]. Zenodo. https://doi.org/10.5281/zenodo.10976245

Fan, J. (2024b). Physics Informed Neural Networks with New Activation Function. Zenodo. https://doi.org/10.5281/zenodo.10976302

Goodfellow, I., Bengio, Y., Courville, A., Goodfellow, I., Bengio, Y., & Courville, A. (2016). Deep Learning Introduction. Cambridge: Mit Press.

He, Q. Z., Barajas-Solano, D., Tartakovsky, G., & Tartakovsky, A. M. (2020). Physics-informed neural networks for multiphysics data assimilation with application to subsurface transport. Advances in Water Resources, 141, 15. https://doi.org/10.1016/j.advwatres.2020.103610

Hunter, J. D. (2007). Matplotlib: A 2d graphics environment. Computing in Science & Engineering, 9(3), 90–95. https://doi.org/10.1109/MCSE.2007.55

Jackson, T., Mansfield, K., Saafi, M., Colman, T., & Romine, P. (2008). Measuring soil temperature and moisture using wireless MEMS sensors. Measurement, 41(4), 381-390. https://doi.org/10.1016/j.measurement.2007.02.009

Kamai, T., Tuli, A., Kluitenberg, G. J., & Hopmans, J. W. (2008). Soil water flux density measurements near 1 cm d⁻¹ using an improved heat pulse probe design. Water Resources Research, 44, 12. https://doi.org/10.1029/2008wr007036

Karniadakis, G. E., Kevrekidis, I. G., Lu, L., Perdikaris, P., Wang, S., & Yang, L. (2021). Physics-informed machine learning. Nature Reviews Physics, 3(6), 422-440. https://doi.org/10.1038/s42254-021-00314-5

Raissi, M., & Karniadakis, G. E. (2018). Hidden physics models: Machine learning of nonlinear partial differential equations. Journal of Computational Physics, 357, 125-141. https://doi.org/10.1016/j.jcp.2017.11.039

Raissi, M., Perdikaris, P., & Karniadakis, G. E. (2019). Physics-informed neural networks: A deep learning framework for solving forward and inverse problems involving nonlinear partial differential equations. Journal of Computational Physics, 378, 686-707. https://doi.org/10.1016/j.jcp.2018.10.045

Raissi, M., Yazdani, A., & Karniadakis, G. E. (2020). Hidden fluid mechanics: Learning velocity and pressure fields from flow visualizations. Science, 367(6481), 1026-+. https://doi.org/10.1126/science.aaw4741

Robinson, D. A., Campbell, C. S., Hopmans, J. W., Hornbuckle, B. K., Jones, S. B., Knight, R., Wendroth, O. (2008). Soil moisture measurement for ecological and hydrological watershed-scale observatories: A review. Vadose Zone Journal, 7(1), 358-389. https://doi.org/10.2136/vzj2007.0143

Sadeghi, M., Ebtehaj, A., Crow, W. T., Gao, L., Purdy, A. J., Fisher, J. B., . . . Tuller, M. (2020). Global Estimates of Land Surface Water Fluxes from SMOS and SMAP Satellite Soil Moisture Data. Journal of Hydrometeorology, 21(2), 241-253. https://doi.org/10.1175/jhm-d-19-0150.1

Saito, H., Simunek, J., & Mohanty, B. P. (2006). Numerical analysis of coupled water, vapor, and heat transport in the vadose zone. Vadose Zone Journal, 5(2), 784-800. https://doi.org/10.2136/vzj2006.0007

Scanlon, B. R., Keese, K., Reedy, R. C., Simunek, J., & Andraski, B. J. (2003). Variations in flow and transport in thick desert vadose zones in response to paleoclimatic forcing (0-90 kyr): Field measurements, modeling, and uncertainties. Water Resources Research, 39(7), 18. https://doi.org/10.1029/2002wr001604

Shen, C., Appling, A. P., Gentine, P., Bandai, T., Gupta, H., Tartakovsky, A., . . . Lawson, K. (2023). Differentiable modelling to unify machine learning and physical models for geosciences. Nature Reviews Earth & Environment, 4(8), 552-567. https://doi.org/10.1038/s43017-023-00450-9

Song, W., Shi, L., Wang, L., Wang, Y., & Hu, X. (2022). Data-Driven Discovery of Soil Moisture Flow Governing Equation: A Sparse Regression Framework. Water Resources Research, 58(8). https://doi.org/10.1029/2022wr031926

Tartakovsky, A. M., Marrero, C. O., Perdikaris, P., Tartakovsky, G. D., & Barajas-Solano, D. (2020). Physics-Informed Deep Neural Networks for Learning Parameters and Constitutive Relationships in Subsurface Flow Problems. Water Resources Research, 56(5), 16. https://doi.org/10.1029/2019wr026731

Umutoni, L., & Samadi, V. (2024). Application of machine learning approaches in supporting irrigation decision making: A review. Agricultural Water Management, 294, 108710. https://doi.org/10.1016/j.agwat.2024.108710

Vangenuchten, M. T. (1980). A CLOSED-FORM EQUATION FOR PREDICTING THE HYDRAULIC CONDUCTIVITY OF UNSATURATED SOILS. Soil Science Society of America Journal, 44(5), 892-898. https://doi.org/10.2136/sssaj1980.03615995004400050002x

Wang, N. Z., Zhang, D. X., Chang, H. B., & Li, H. (2020). Deep learning of subsurface flow via theory-guided neural network. Journal of Hydrology, 584, 24. https://doi.org/10.1016/j.jhydrol.2020.124700

Wang, Y., Shi, L., Hu, X., Song, W., & Wang, L. (2023). Multiphysics-Informed Neural Networks for Coupled Soil Hydrothermal Modeling. Water Resources Research, 59(1). https://doi.org/10.1029/2022wr031960

Wythoff, B. J. (1993). Backpropagation neural networks: a tutorial. Chemometrics and Intelligent Laboratory Systems, 18(2), 115-155.

https://doi.org/10.1016/0169-7439(93)80052

Yan, X., Song, X., Wang, Y., Wang, W., Cheng, Q., Yang, X., & Du, T. (2023). A pipeline robot system for monitoring soil water content distribution. Journal of Hydrology, 620. https://doi.org/10.1016/j.jhydrol.2023.129526

Yang, L., Treichler, S., Kurth, T., Fischer, K., Barajas-Solano, D., Romero, J., Ieee. (2019, Nov 17). Highly-scalable, physics-informed GANs for learning solutions of stochastic PDEs. Paper presented at the 3rd IEEE/ACM Workshop on Deep Learning on Supercomputers (DLS), Denver, CO. https://doi.org/10.1109/DLS49591.2019.00006

Yang, Y. B., & Perdikaris, P. (2019). Adversarial uncertainty quantification in physics-informed neural networks. Journal of Computational Physics, 394, 136-152. https://doi.org/10.1016/j.jcp.2019.05.027

Yazdchi, M., Khalili, N., & Valliappan, S. (1999). Dynamic soil–structure interaction analysis via coupled finite-element–boundary-element method. Soil Dynamics and Earthquake Engineering, 18(7), 499-517. https://doi.org/10.1016/S0267-7261(99)00019-6

Yu, S., Xu, Q., Cheng, X., Xiang, Y., Zhu, Y., Yan, X., . . . Cheng, Q. (2021). In-situ determination of soil water retention curves in heterogeneous soil profiles with a novel dielectric tube sensor for measuring soil matric potential and water content. Journal of Hydrology, 603, 126829. https://doi.org/https://doi.org/10.1016/j.jhydrol.2021.126829

Zhang, Y., & Yang, Q. (2018). An overview of multi-task learning. National Science Review, 5(1), 30-43. https://doi.org/10.1093/nsr/nwx105

Zhao, W. L., Gentine, P., Reichstein, M., Zhang, Y., Zhou, S., Wen, Y. Q., . . . Qiu, G. Y. (2019). Physics-Constrained Machine Learning of Evapotranspiration. Geophysical Research Letters, 46(24), 14496-14507. https://doi.org/10.1029/2019gl085291

Zhu, Y. H., Zabaras, N., Koutsourelakis, P. S., & Perdikaris, P. (2019). Physics-constrained deep learning for high-dimensional surrogate modeling and uncertainty quantification without labeled data. Journal of Computational Physics, 394, 56-81. https://doi.org/10.1016/j.jcp.2019.05.024